Changes in LXRα phosphorylation promote a novel diet-induced transcriptome that alters the transition from fatty liver to steatohepatitis

Natalia Becares[1], Matthew C Gage[1], Lucia Martin Gutierrez[1], Benoit Pourcet[1]#, Oscar M Pello[1], Tu Vinh Luong[2], Saioa Goñi[3], Ning Liang[3], Cesar Pichardo[4], Elina Shrestha[5], Hanne-Røberg-Larsen[6], Vanessa Diaz[4], Knut R. Steffensen[7], Michael J. Garabedian[5], Krista Rombouts[8], Eckardt Treuter[3], Inés Pineda-Torra[1]

[1] Centre for Clinical Pharmacology, Division of Medicine, University College of London, 5 University Street, London, WC1 E6JF, United Kingdom.

[2] Department of Cellular Pathology, University College London, Royal Free Campus, Rowland Hill Street, London, NW3 2PF, United Kingdom

[3] Karolinska Institute, Department of Biosciences and Nutrition, S-14157 Huddinge, Sweden

[4] Department of Mechanical Engineering, University College London, Roberts Building, 1-19 Torrington Place, London, WC1E 7JE, United Kingdom

[5] Department of Microbiology, New York University School of Medicine, New York, New York 10016, United States of America

[6] Department of Chemistry, University of Oslo, Sem Saelandsvei 26, 0371 Oslo, Norway

[7] Division of Clinical Chemistry, Department of Laboratory Medicine, Karolinska Institut, Huddinge, Sweden

[8] Institute for Liver & Digestive Health, University College London, Royal Free, London, NW3 2PF, United Kingdom

Correspondence should be addressed to:

Inés Pineda-Torra, Centre for Clinical Pharmacology, Division of Medicine, University College London, London WC1E6JF, UK. Phone: +44 (0)20 7679 6535. Fax: +44 (0)20 7679 6211. E-mail: i.torra@ucl.ac.uk

New address: European Genomic Institute for Diabetes, FR 3508, F-59000 Lille, France; Univ. Lille, F-59000 Lille, France; INSERM UMR 1011, F-59000 Lille, France; Institut Pasteur de Lille, F-59000 Lille, France.

SUMMARY

Understanding the transition from fatty liver or steatosis to more advanced inflammatory and fibrotic stages of non-alcoholic fatty liver disease (steatohepatitis), is key to define strategies that alter or even reverse the progression of this pathology. The Liver X Receptor alpha (LXRα) controls hepatic lipid homeostasis and inflammation. Here we show that mice carrying a mutation that abolishes phosphorylation at Ser196 (S196A) in LXRα exhibit reduced hepatic inflammation and fibrosis when challenged with a high fat-high cholesterol diet, despite displaying enhanced hepatic lipid accumulation. This protective effect is associated with reduced cholesterol accumulation, a key promoter of lipid-mediated hepatic damage. Reduced steatohepatitis in S196A mice involves the reprogramming of the liver transcriptome by promoting diet-induced changes in the expression of genes involved in endoplasmic reticulum stress, extracellular matrix remodelling, inflammation and lipid metabolism. Unexpectedly, changes in LXRα phosphorylation uncover novel diet-specific target genes, whose regulation does not simply mirror ligand-induced LXR activation. These unique LXRα phosphorylation-sensitive, diet-responsive target genes are revealed by promoting LXR occupancy and cofactor recruitment in the context of a cholesterol-rich diet. Therefore, LXRα phosphorylation at Ser196 critically acts as a novel nutritional sensor that promotes a unique diet-induced transcriptome thereby modulating metabolic, inflammatory and fibrotic responses important in the transition to steatohepatitis.

INTRODUCTION

Non-Alcoholic Fatty Liver Disease (NAFLD) is a condition that represents a wide spectrum of liver diseases, ranging from simple fatty liver (steatosis), steatosis accompanied by inflammation with or without fibrosis (steatohepatitis or NASH) that can progress to necrosis, cirrhosis and hepatocellular carcinoma promoting liver-related mortality (Bellentani et al., 2010). In this condition, fatty liver is characterized by hepatic triglyceride and free cholesterol accumulation in the absence of significant alcohol consumption. NAFLD is strongly associated with obesity, insulin resistance and type 2 diabetes (Gaggini et al., 2013) and its prevalence in Western Countries is estimated to affect 20-30% of the adult population (Bellentani et al., 2010). Steatosis alone is considered relatively benign. It is the transition to NASH that represents a key step into further liver damage and mortality, which without intervention leads to organ transplantation (Musso et al., 2011). However, the mechanisms underlying this transition are poorly understood. Most therapies for NAFLD have focused on preventing progression of fatty liver or reversing established inflammatory or fibrotic states (EASL et al., 2016). Therapies such as insulin sensitizers, or lipid-lowering drugs are not aimed at treating NAFLD directly, but rather its associated conditions and thus, only display limited efficacy. Indeed, currently the recommended therapy for NAFLD is weight loss through lifestyle modifications (Thoma et al., 2012). Therefore, identifying factors that modulate the transition from fatty liver to NASH is crucial for the development of therapies directly targeting NAFLD.

The Liver X Receptor (LXR) lipid-activated transcription factors, LXRα (NR1H3) and LXRβ (NR1H2), act as heterodimers with the Retinoid X Receptor, RXR (NR2B1, NR2B2 and NR2B3) to critically regulate cholesterol and fatty acid homeostasis (Peet et al., 1998; Repa et al., 2000a). In addition, LXRs act as global modulators of inflammation and immunity (Steffensen et al., 2013; Tall and Yvan-Charvet, 2015). Specifically in liver, they have demonstrated anti-inflammatory and anti-fibrotic activities in models of acute liver disease (Beaven et al., 2011; Hamilton et al., 2016). Besides ligand binding, LXR activity can be modulated by post-translational modifications (Becares et al., 2016). Specifically, we and others previously showed that LXRα is phosphorylated at Ser196 (Ser198 in the human homolog) in macrophages (Chen et al., 2006; Torra et al., 2008; Wu et al., 2015) and that ligand-induced LXRα phosphorylation at this site alters its activity in a gene-specific manner (Torra et al., 2008; Wu et al., 2015).

Despite previous reports showing LXRα phosphorylation in this and other residues (Cho et al., 2015; Hwahng et al., 2009; Yamamoto T et al., 2007), the physiological consequences of changes in LXRα phosphorylation remain unknown. Here, we identify global LXRα phosphorylation deficiency at Ser196 as a nutritional sensor affecting hepatic lipid metabolism and the development of hepatic inflammation and fibrosis in a dietary model of NAFLD. Mice expressing a whole-body Ser to Ala mutant of LXRα disrupting phosphorylation at Ser196 (S196A) exhibit attenuated

hepatic inflammation and fibrosis despite showing pronounced hepatic steatosis. This protective effect of the LXRα mutant is associated with reduced levels of factors promoting lipid-mediated hepatic damage. Moreover, the LXRαS196A mutant reveals novel phosphorylation-sensitive target genes predominantly in response to a cholesterol-rich diet. Therefore, disruption of LXRα phosphorylation at Ser196 critically impacts the transition to diet-induced steatohepatitis.

RESULTS AND DISCUSSION

LXRα is phosphorylated at Ser198/196 in liver and LXRα-S196A mice exhibit more pronounced steatosis

We previously showed that LXRα is phosphorylated at Ser198 in a motif not found in the LXRβ isotype (Fig. S1A) in a murine macrophage-like cell line overexpressing the human LXRα receptor (Torra et al., 2008; Wu et al., 2015). We now demonstrate that LXRα is phosphorylated in liver in both mice (Fig. 1A) and human liver (Fig. S1B). To understand the impact of LXRα phosphorylation in physiology, we generated a global knock-in mouse carrying a homozygous serine-to-alanine mutation at the LXRα-Ser196 residue (S196A) under the PGK-1 promoter, which impairs LXRα phosphorylation at S196 (Fig. 1A and S1C-E). S196A mice have no apparent dysmorphic phenotypes, their developmental growth is similar to their matching wild-type controls (WT) (not shown) and no significant changes in hepatic lipids or other metabolic parameters exist between groups when fed a chow diet (Table S1). This indicates LXRα phosphorylation deficiency has little effect in the metabolic response of a diet devoid of cholesterol.

Cholesterol metabolites are known LXR endogenous ligands (Janowski et al., 1996; Lehmann et al., 1997) and diets with a high cholesterol content enhance LXR activity *in vivo* (Kalaany et al., 2005). Given that cholesterol induces LXRα phosphorylation (Torra et al., 2008), we hypothesised that LXRα phospho-mutant animals respond differently to a High Fat-High Cholesterol (HFHC) diet (Savard et al., 2013) compared to matching WT mice. Total body weight, plasma insulin and glucose levels were similar between S196A and WT mice fed a HFHC diet (Table S2). Previous studies have extensively shown the importance of LXRα on hepatic steatosis (Peet et al., 1998; Zhang et al., 2012). Remarkably, and in contrast to plasma levels (Fig. S1F), hepatic Non-Esterified Fatty Acids (NEFAs) and triglyceride levels in S196A mice were about 80% and 40% higher respectively, than in WT mice (Fig. 1B). Consistently, S196A mice have enhanced micro and macrovesicular steatosis (Fig. 1C, D). Further characterization of lipid droplet area revealed that mutant mice exhibit larger and more numerous lipid droplets (Fig. 1E), confirming their predominant macrovesicular steatosis, which is accompanied by an enhanced expression of lipid droplet genes (Fig. S1G).

Increased steatosis in S196A mice was also associated with enhanced hepatic expression of the *Srebp1c* lipogenic transcription factor, and other well-established LXR target genes involved in fatty acid synthesis (fatty acid synthase, *Fas*) and desaturation (stearoyl-CoA desaturase-1, *Scd-1*) (Fig. 1F). In contrast, expression of genes involved in fatty acid elongation (*Elovl6*) or uptake (*Cd36*), were not affected suggesting LXRα phosphorylation alters gene expression in a gene specific manner confirming our previous findings in macrophages (Torra et al., 2008; Wu et al., 2015). Given that plasma NEFAs, TGs and insulin levels do not differ between genotypes (Fig. S1F and Table S2), differences in hepatic fat accumulation in S196A mice are likely to result from an enhanced lipogenic programme as observed in other LXR models (Fungwe et al., 1994; Grefhorst et al., 2002; Schultz et al., 2000). Altogether, these results demonstrate that LXRα phosphorylation deficiency at S196 induces hepatic steatosis in response to a HFHC diet.

Impaired LXRα phosphorylation attenuates diet-induced hepatic inflammation and fibrosis

Diet-induced hepatic steatosis precedes inflammation and progression to fibrosis in experimental models (Sanyal, 2005). Strikingly, despite the increased steatosis, LXRα-S196A mice displayed less inflammation (Fig. 2A) and significantly less collagen deposition than their WT counterparts (Fig. 2B). This was associated with a significant decrease in the expression of several pro-inflammatory and pro-fibrotic mediators, such as *Osm* (Znoyko et al., 2005), *Cxcl1* (Semba et al., 2013) and *Spp1* (Syn et al., 2011) as well as genes involved in collagen synthesis (*Col1a1* and *Tgfb2*) (Fig. 2C). Only a subset of the genes analysed was affected by changes in LXRα phosphorylation (Fig. 2C and not shown) corroborating the gene specific effects this modification has on LXRα-modulated gene expression. Interestingly, changes in response to the cholesterol-rich diet further evidenced the attenuated inflammatory and fibrotic response of the S196A mice (Fig. 2D). For instance, basal expression of pro-fibrotic *Spp1* is reduced in S196A mice and is only minimally enhanced when challenged with this diet. Equally, for other genes examined, differences between genotypes were only revealed upon exposure to the HFHC diet (Fig. 2D).

To further characterize this differential hepatic inflammation and fibrosis, we next investigated pathways implicated in the pathogenesis of lipid-induced liver damage. The number of apoptotic cells present was similar between genotypes (Fig. S2A), as were lipid peroxidation levels (Fig. S2B) and hepatic macrophage content (Fig. S2C). Endoplasmic reticulum (ER) stress is an adaptive mechanism allowing cells to survive upon physiological changes that require different rates of protein folding. It is particularly important in cells with a high ER content, such as hepatocytes. The link between ER stress and hepatic damage has been extensively studied and it is now understood that prolonged ER stress not only increases steatosis levels but also promotes hepatic fibrosis (Dara et al., 2011). Interestingly, expression of several factors involved in the activation of ER stress such as the UPR target gene C/EBP homologous protein (Chop) and the Activating Transcription Factor (Atf3) (Lebeaupin et al., 2015) was reduced in S196A mice (Fig.

2E), suggesting these animals could be protected from lipotoxicity through a reduction in ER stress activation. This was further supported by a significant decrease in the splicing of X-box-binding protein-1 (XBP1) mRNA ER stress marker (Fig. 2E).

Overall, these findings demonstrate that blocking LXRα-phosphorylation at S196 attenuates lipid-induced hepatic inflammation and fibrosis despite the enhanced steatosis.

LXRα phospho-mutant mice are protected from dietary cholesterol accumulation

Several animal studies have demonstrated that cholesterol can act as a hepatotoxic agent (Marí et al., 2006) and activates hepatic stellate cells, key mediators in collagen deposition in hepatic fibrosis (Tomita et al., 2014). In contrast to WT, plasma total cholesterol levels in S196A mice challenged with a HFHC diet remained unchanged, showing approximately 60% less plasma total cholesterol than WT animals (Fig. 3A). In parallel, liver to body weight ratio in S196A mice was 20% smaller compared to WT controls (Table S2), possibly reflecting the markedly reduced hepatic total cholesterol accumulation in these animals (Fig. 3B). In light of these findings, we next investigated cholesterol metabolism pathways (uptake, catabolism and export), that could be altered by the phospho-mutant LXRα receptor, some of which are already well-characterised targets of LXRα (Laffitte et al., 2001; Repa et al., 2000b, 2002; Venkateswaran et al., 2000). Expression of *Abcg1* and *Abca1*, responsible for cholesterol efflux into mature High Density Lipoproteins (HDL) and lipid-poor apolipoproteins respectively, were decreased in S196A mice (Fig. 3C). These transporters are key mediators of the Reverse Cholesterol Transport that promotes the traffic of cholesterol from lipid-loaded cells in the periphery back to the liver to be excreted. Notably, expression of transporters implicated in hepatobiliary cholesterol secretion *Abcg5* (Wu et al., 2004), and to a lower extent *Abcg8*, were increased in the S196A mice (Fig. 3C), which could explain the reduced hepatic total cholesterol levels in these mice.

Moreover, intracellular cholesterol accumulation is thought to lead to activation of the unfolded protein response pathway in the ER (Devries-Seimon et al., 2005), inhibiting protein transport to the Golgi (Kockx et al., 2012) to adapt cells to a changing environment and re-establish ER function. One gene linking cholesterol metabolism and ER stress is *Tm7sf2*. In addition to participating in cholesterol biosynthesis as a 3β-hydroxysterol Δ14-reductase, *Tm7sf2* acts as an ER sensor and modulates the ensuing inflammatory response by triggering anti-inflammatory pathways (Bellezza et al., 2013). Consistent with a decreased ER stress response and hepatic inflammation in S196A mice, *Tm7sf2* expression is significantly enhanced in S196A mice exposed to the diet (Fig. S2D). Importantly, other genes coding for cholesterol biosynthesis enzymes remain largely unaffected suggesting that cholesterol modulation of ER stress responses, rather than cholesterol biosynthesis itself, is altered in S196A mice. No difference was observed in the levels of genes involved in cholesterol intestinal absorption and excretion (Fig. S2E), an important means

by which LXR controls cholesterol homeostasis (Bonamassa and Moschetta, 2013); nor in the expression of other nuclear receptors regulating lipid metabolism (Fig. S2F and data not shown). Overall, these findings suggest the reduced cholesterol accumulation seen in the S196A mice is most likely due to an increased hepatobiliary secretion of cholesterol.

Analysis of hepatic gene expression in response to the HFHC diet revealed that while *Abcg1* levels are severely induced by the diet in both groups, enhanced *Abcg5* expression by the diet is specific to the S196A genotype (Fig. 3D) further demonstrating how different diet responses are between genotypes. Interestingly, expression of these genes was only affected by LXR phosphorylation on the experimental diet, consistent with cholesterol content being similar in WT and S196A groups on chow (Table S1). As expected, hepatic expression of the cholesterogenic transcription factor *Srebp2* and its target gene *Ldlr* in WT mice was strongly repressed upon addition of dietary cholesterol (Fig. 3E). In contrast, these genes were largely unaffected by the diet in S196A mice, mirroring the unchanged levels of hepatic cholesterol in these animals in response to diet (Fig. 3A). Moreover, LXRα phospho-mutant mice also showed significantly reduced levels of plasma oxysterols (Fig. 3F), some of which act as LXR ligands and have been reported to be enhanced in patients with NAFLD (Ikegami et al., 2012). This is associated with changes in the expression of Cyp7b1 (Fig. 3C), an enzyme involved in oxysterol catabolism (Uppal et al., 2007), while enzymes implicated in their synthesis are unaffected (not shown). Overall, these data show that S196A mice respond significantly different to a HFHC diet, suggesting LXRα phosphorylation acts as a novel molecular sensor of dietary cholesterol in the progression to hepatic inflammation and fibrosis.

Impaired LXRα phosphorylation reprograms hepatic gene expression and uncovers a novel diet-modulated LXRα transcriptome

To better understand the extent of the disparity in diet-induced responses between WT and S196A mice and to identify novel pathways sensitive to LXRα phosphorylation, we next assessed genome-wide transcriptomic differences by RNAseq analysis (Fig. S3A). This revealed 667 genes whose hepatic expression is significantly altered in the phospho-mutant mice fed a HFHC diet (205 being upregulated and 127 downregulated with a fold difference ≥1.5) (Fig. 4A). Confirming our initial findings, pathway enrichment analysis showed a remarkable induction of genes involved in different lipid metabolism pathways (Fig. 4B,C), as well as a robust decrease in wound healing and fibrotic mediators (Fig. 4B,D). Amongst these, eleven collagen species, and importantly, Lysyl oxidase (LOX) and lysyl oxidase-like proteins (LOXLs) responsible for collagen stabilisation through irreversible crosslinking (Kanta, 2016; Liu et al., 2016) were altered. This is the first time this class of enzymes, recently reported to promote fibrosis progression and limit its reversibility (Liu et al., 2016) have been linked to LXRα.

When comparing gene expression changes in response to diet (chow vs HFHC for each genotype), the number of genes affected varied substantially between WT and S196A mice (Fig. S3B), further supporting that impaired phosphorylation of LXRα at Ser196 alters the susceptibility to diet-induced hepatic injury by reprogramming hepatic transcriptomes. Moreover, the expression of a subset of genes that distinguish between low-risk/mild and high-risk/severe NAFLD amongst pre-symptomatic patients (Moylan et al., 2014) is remarkably different in WT and S196A mice (Fig. 4E). This further suggests changes in LXRα phosphorylation may alter NAFLD progression. Most of these genes are involved in extracellular matrix remodelling and tissue regeneration, emphasizing a role for Ser196 LXRα phosphorylation in the regulation of these pathways.

Genes with the strongest difference in expression between genotypes were confirmed in a separate set of animals (Fig. 4F and S3C). Importantly, the majority of these genes are only modulated by LXRα phosphorylation status in a cholesterol-rich environment (Fig. S3D and not shown) and have not been reported to be subject to LXR regulation in liver, thus highlighting the relevance of LXRα phosphorylation in modulating transcriptional responses to dietary cholesterol. One such gene, *Ces1f*, is a member of the carboxylesterase 1 (Ces1) family of enzymes that hydrolyse cholesterol esters and triglycerides and control hepatic lipid mobilization (Quiroga et al., 2012; Zhao et al., 2005). While previous studies failed to show *Ces1f* regulation by LXR ligands (Jones et al., 2013), our findings demonstrate *Ces1f* is preferentially sensitive to the phospho-mutant LXRα on a cholesterol-rich environment (Fig. 4F and S3D,E). Ces1 was recently linked with protection against liver inflammation and injury (Xu et al., 2016) and its hepatic deficiency strongly increases susceptibility to cholesterol-driven hepatic injury (Li et al., 2017). However, the specific contribution by *Ces1f* in NAFLD progression has not been addressed, possibly due to the high sequence similarity shared by Ces genes. In addition to *Ces1f*, other Ces1 members are differentially regulated by the LXRα phospho-mutant (*Ces1b, Ces1c, Ces1d, Ces1e*), most of which are only revealed to be sensitive to LXRα phosphorylation in a cholesterol-rich environment (Fig S3E). Interestingly, the form previously shown to be regulated by LXR ligands in liver, *Ces2c*, (Jones et al., 2013) does not vary in S196A mice regardless of the diet used (Fig S3E), again pointing at unique differences in the transcriptional response exerted by changes in LXRα phosphorylation upon exposure to a high-cholesterol diet.

Identification of DR4 sequences in novel dual LXRα phosphorylation/diet sensitive genes

In silico analysis of the *Ces1f* gene uncovered a degenerated DR4 sequence resembling the published consensus LXRE (Boergesen et al., 2012) that was preferentially bound by LXR in HFHC-fed S196A liver (Fig. 4G). This was associated with increased RNA Polymerase II (Pol II) and phosho-Ser2 Pol II (pSer-Pol II) occupancy to the *Ces1f* transcription start site reflecting an enhanced transcriptional initiation and elongation of the *Ces1f* transcript respectively (Fig. S3G). By comparison, binding of the LXR heterodimerisation partner RXR to the *Ces1f* DR4 sequence

was not affected (Fig. 4G). A similar binding pattern was observed for another DR4 sequence identified in the *Cyp2c69* gene, whose expression is enhanced by about 5-fold in LXRα-S196A mice (Fig. 4H and S3H). In contrast, occupancy by both LXR and RXR to the well-established LXRE in the *Srebp-1c* promoter was induced (Fig. 4I), as was Pol II and pSer-Pol II (Fig. S3I). This suggests that impaired LXRα phosphorylation at S196 allows transcriptional activation of a subset of genes containing degenerated DR4 sequences (*i.e*. *Ces1f, Cyp2c69*) without affecting RXR occupancy.

It is important to note these novel sequences were revealed by homology to previously reported LXR binding sites given that there are currently no available genome-wide LXR binding analyses interrogating responses to diet, which may not necessarily phenocopy binding patterns identified upon activation by synthetic ligands (Boergesen et al., 2012). Indeed, ChIP-seq analysis in WT mouse livers treated with the LXR specific ligand GW3965 shows very little or no presence of LXR at the *Ces1f* and *Cyp2c69* DR4 sequences identified *in silico* (not shown), further supporting that both phosphorylation status of LXRα and diet environment are critical for the regulation of these genes. Certain members of the Ces family are modulated by nuclear receptors such as PPARα (Jones et al., 2013). Because the hepatic expression of PPARα is not substantially altered in S196A mice (Fig. S2F) and no PPARα binding was observed on the identified Ces1f and Cyp2c69 sequences based on reported ChIP-seq analysis of PPARα binding sites (Boergesen et al., 2012), it is unlikely this nuclear receptor participates in the regulation of Ces1f and Cyp2c69 expression by the LXRα mutant under our experimental conditions.

Molecular modelling studies suggest that phosphorylation of LXRα at S198 (murine S196) induces a structural change in the hinge region of the receptor (Torra et al., 2008; Wu et al., 2015), which can affect not only ligand binding but also cofactor recruitment (Pawlak et al., 2012). Our previous studies in macrophages showed that, upon ligand activation, this modification affects the transcriptional activity of LXRα by modulating cofactor recruitment including the corepressor NCoR (Torra et al., 2008; Wu et al., 2015). However, we were unable to detect differences in NCoR occupancy between genotypes in livers from HFHC-fed mice (not shown), suggesting responses to cholesterol *in vivo* may involve other transcriptional players. Indeed, binding of TBLR1, which participates in nuclear receptor cofactor exchange (Perissi et al., 2004) and modulates LXR target gene expression in hepatic cell lines (Jakobsson et al., 2009), was identified to preferentially interact with LXRα S196A by proteomic analysis (Fig. S3F). Consistently, TBLR1 occupancy was significantly enhanced in S196A livers exposed to the HFHC diet (Fig. 4G,H,I) suggesting TBLR1 is an important component facilitating the transcription of these genes by the LXRα phospho-mutant. Collectively, these data indicate that disrupting LXRα phosphorylation at Ser196 affects diet-induced responses in liver and reveals LXR target genes through differential binding of LXR and TBLR1 to novel target sequences (Fig. 4J).

CONCLUSIONS

The role of LXRα in promoting fatty acid and triglyceride accumulation is well documented (7) and has proven a major obstacle in the development of LXR ligands as therapeutics against metabolic and cardiovascular disorders. However, recently developed LXR antagonists have been shown to be effective against NAFLD in rodent models (Griffett et al., 2013, 2015). Whether changes in LXRα expression occur during NAFLD progression in humans remains contradictory. On the one hand, LXRα levels were shown to positively correlate with disease progression (Ahn et al., 2014; Lima-Cabello et al., 2011), which could represent either an adaptive or a pathogenic response to ongoing cellular and molecular changes. On the other hand, reports have showed LXRα expression is unaffected during NAFLD (Aguilar-olivos et al., 2015). Moreover, whether modifications in LXRα participate in the progression to steatohepatitis is unknown. Posttranslational modifications are a powerful means by which the activity and function of nuclear receptors can be altered. Despite the key importance of certain nuclear receptors in maintaining metabolic homeostasis, our understanding of how these modifications impact on metabolic diseases is scarce (Becares et al., 2016). To date, the physiological consequences of LXRα phosphorylation, sumoylation and acetylation have only been studied *in vitro* or non-specifically in animal models by pharmacologically or genetically altering the enzymes enhancing or inhibiting these modifications (Becares et al., 2016).

In this study, we report for the first time that non-pharmacological modulation of LXRα affects diet-induced responses in liver by attenuating early signs of steatohepatitis in the presence of abundant lipid accumulation. Using a novel mouse model harbouring an S196A mutation that disrupts LXRα phosphorylation at Ser196, we demonstrate that genetic impairment of LXRα phosphorylation at this residue dictates the response to a HFHC diet that promotes early stages of NAFLD. Additionally, this is the first study to show the phosphorylation of LXRα at this residue in human liver. Disrupting LXRα phosphorylation at Ser196 also reveals unique LXR target genes through differential binding of LXR and TBLR1 to novel target sequences. Overall, LXRα phosphorylation at Ser196 critically acts as a novel nutritional sensor that promotes a unique diet-induced transcriptome and modulates metabolic, inflammatory and fibrotic responses that are key in NAFLD progression.

EXPERIMENTAL PROCEDURES

Generation of the S196A transgenic animal models

The S196A floxed ($S196A^{fl/fl}$) mouse line was generated by Ozgene Pty Ltd (Bentley WA, Australia). The genomic sequence for the murine LXRα (Nr1h3) gene was obtained from the

Ensembl Mouse Genome Server (http://www.ensembl.org/Mus_musculus/), Ensembl gene ID: ENSMUSG00000002108. The mutant fragment, located on Exon 5, contains a serine-to-alanine mutation at Ser196 introduced by site-directed mutagenesis. The point-mutant exon was delivered into an intronic site inside the targeting vector, placed in opposite orientation and thus without coding capacity (Fig. S1A). The targeting construct was electroporated into the Bruce4 C57BL/6 ES cell line. Homologous recombinant ES cell clones were identified by Southern hybridization and injected into BALB/cJ blastocysts. Male chimeric mice were obtained and crossed to C57BL/6J females to establish heterozygous germline offsprings on a pure C57BL/6 background. The germline mice were crossed to a FLP Recombinase mouse line (Takeuchi et al., 2002) to remove the FRT flanked selectable marker cassette (Flp'd mice). Flp'd mice were then crossed with a transgenic C57BL/6 mouse strain carrying a Cre recombinase under the PGK-1 promoter (Koentgen et al., 2010), resulting in the inversion and insertion of the lox-flanked mutated (loxP) vector exon 5 region in the sense orientation, and deletion of the wild-type (WT) sequence in most adult cell lineages (S196A mice) while WT matching controls carry the WT sequence in the sense orientation (Fig. S1D). Mice were genotyped by PCR analysis of ear biopsies (Fig S1D,E) using the Jumpstart Taq DNA Polymerase (Sigma Aldrich) and the following primers: wild-type (WT) forward 5'GGTGTCCCCAAGGGTGTCCT, reverse 5' AAGCATGACCTGCACACAAG and mutant forward 5' GGTGTCCCCAAGGGTGTCCG. Animals were housed together and maintained in a pathogen-free animal facility in a 12-h light-dark cycle. All procedures were carried under the UK's Home Office Animals (Scientific Procedures) Act 1986.

Diet studies and tissue collection

Ten-week old WT and S196A female mice were fed ad libitum a High Fat-High Cholesterol (HFHC) diet (17,2% Cocoa Butter, 2,8% Soybean Oil, 1,25% Cholesterol, 0,5% Sodium Cholate; AIN-76A/Clinton Diet #4, Test Diet Limited, UK) or a chow diet (18% Protein, 6.2% Fat, 0% Cholesterol; Harlan Laboratories) for 6 weeks. Mice were fasted overnight prior to sacrifice. Blood was collected by cardiac puncture and plasma was aliquoted and frozen at -80 °C. Tissue was dissected, weighted and frozen at -80 °C or placed in RNAlater (Sigma Aldrich).

Plasma and hepatic lipid determination

Frozen livers (50 mg) were homogenized in 250 mM sucrose, 2 mM EDTA, 10 mM Tris buffer using ceramic beads in a Minilys Tissue Homogenizer (Bertin Corp.). Triglycerides and Cholesterol were extracted with Isopropanol or Chloroform:Methanol (1:1) solutions, respectively. Non Esterified Free Fatty Acids (NEFAs) were extracted by incubating liver homogenates with 1% Triton-100X and chloroform solution. Plasma and hepatic total cholesterol, triglyceride levels (Wako Diagnostics), and NEFAs (Abcam) were determined by colorimetric enzymatic assay kits as per the manufacturer's recommendations. Hepatic lipid content was normalized to protein concentration.

Oxysterol LC-MS analysis

Protein was precipitated from plasma with 480 pM of the appropriate internal standards (Avanti Polar Lipids, Alabaster, AL, USA). Sample clean-up was conducted off-line, using solid phase extraction (SPE, SilactSPE C18 100 mg, Teknolab, Ski, Norway) and dryed at 30 °C, re-dissolved in 2-propanol and treated as described (Roberg-Larsen et al., 2014). Samples and calibration solutions were analysed using an Ultimate 3000 UHPLC connected to an Advantage QqQ (both Thermo Fisher, Waltham, MA, USA) equipped with an Automatic filtration and filter back-flush SPE add-on, as described (Roberg-Larsen et al., 2016).

RNA extraction and quantification.

Total RNA from was extracted with TRIzol Reagent (Invitrogen). Sample concentration and purity was determined using a NanoDrop™ 1000 Spectrophotometer and cDNA was synthesized using the qScript cDNA Synthesis Kit (Quanta). Specific genes were amplified and quantified by quantitative PCR (qPCR), using the PerfeCTa SYBR Green FastMix (Quanta) on an MX3000p system (Agilent). Primer sequences are available upon request The relative amount of mRNAs was calculated using the comparative Ct method and normalized to the expression of cyclophilin (Pourcet et al., 2016). Mouse Cytokines & Chemokines RT2 Profiler PCR Arrays were performed per the manufacturer's instructions (Qiagen). Briefly, cDNA was synthesized using an RT^2 HT first strand kit (Qiagen), and qPCR analysis was performed using RT2 SYBR Green ROX™ qPCR Mastermix (Qiagen). The relative amount of mRNAs was calculated using the comparative Ct method and normalized to an average of five housekeeping genes. The full list of genes analysed with these arrays can be found at Qiagen's website.

Protein isolation, immunoprecipitation, and immunoblotting

Single cell suspensions from livers were immunoprecipitated with antibodies that specifically recognise human (LXRα, ab41902 Abcam) or murine (LXRα/β) (Pehkonen et al., 2012) receptors previously crosslinked to a column with Protein A/G Agarose following the manufacturer's protocol (Pierce). Phospho-Ser196 specific rabbit polyclonal antibody (Torra et al., 2008, 2009), mouse α-LXRα monoclonal antibody (ab41902, Abcam), α-Hsp90 polyclonal (sc-7947, Santa Cruz) were used for immunoblotting. Anti-rabbit (PO448, Dako) or anti-mouse (NA931VS, GE Healthcare) horseradish-peroxidase-tagged antibodies were used for secondary binding and chemiluminescence (ECL 2 Western Blotting Substrate, Pierce) was used to visualise proteins.

Histopathological analysis

Formalin-fixed, paraffin-embedded mouse livers were cut and stained with hematoxylin and eosin (H&E) or Picrosirius Red (Abcam) dyes. Liver histology was blindly scored by an independent histopathologist based on three semiquantitative items: steatosis (0–3), lobular inflammation (0–3)

and hepatocellular ballooning (0–2) (not shown) (Kleiner et al., 2005; Liang et al., 2014). Stained sections were scanned with NanoZoomer Digital slide scanner (Hamamatsu) and quantification of Picrosirius red-stained areas was performed using Image J on three independent areas per section. Data is represented as the average positively-stained percent of area of interest. Apoptosis was detected in liver tissue sections using a terminal deoxynucleotidyl transferase dUTP nick end-labeling (TUNEL) assay (R&D Systems). Sections were imaged using the Axio Imager.A1 Digital Microscope (Zeiss).

Lipid droplet identification

Identification and quantification of lipid droplets were made with the help of Eli (Easy Lipids) v1.0, an in-house software developed between the Multiscale Cardiovascular Engineering (MUSE) and Dr Pineda-Torra's groups at UCL. This software uses a method based on the Hough Transform (Duda and Hart, 1972) for the identification of the droplets estimating the centres and radii of each of them. A final report is generated with the dimensions of the droplets (i.e. diameter and area) including a histogram describing the frequency of lipid vacuoles within specified diameter ranges. A trial of Eli v1.0 is currently available upon request on the MUSE website at UCL (www.ucl.ac.uk/muse/software).

Lipid peroxidation quantification

Thiobarbituric Acid Reactive Substances (TBARS) were measured in about 25 mg of frozen liver as per manufacturer's instructions (Cayman Chemicals). Briefly, lipid peroxidation was quantified by the reaction of Malondialdehyde (MDA), a product of lipid peroxidation, with thiobarbituric acid (TBA) to form a colorimetric (532 nm) product, proportional to the MDA present. Levels of MDA were normalised to total protein levels, quantified by the Bradford Assay.

LXRα proteomic analysis

HEK293T cells expressing vector only (Vo), FLAG-hLXRα or FLAG-hLXRα-S198A (Shrestha et al., 2016) were treated with 1 μM T0901317 for 8 hours. Purification of protein complexes, Multidimensional Protein Identification Technology, LTQ Mass Spectrometry and analysis was performed as described (Shrestha et al., 2016).

Chromatin Immunoprecipitations

Fresh mouse livers were crosslinked with 2 mM disuccinimidyl glutarate (DSG) for 30 min, followed by 1% formaldehyde for 10 min at room temperature. The reaction was stopped with glycine at a final concentration of 0.125 M for 5 min. Single cell suspension were obtained by grinding liver pieces through a 70 μM cell strainer. Nuclei were isolated as described previously (Fan et al., 2016) and sonicated with the UCD-300 Bioruptor (Diagenode), to generate DNA-fragment sizes of 0.2–0.5 kb. The following antibodies were used for immunoprecipitations: RXRα (sc-553, Santa

Cruz), Pol II (sc-9001, Santa Cruz), Pol II-S2P (ab5095, Abcam) and LXR (Pehkonen et al., 2012). Following RNAse A (Fermentas) and proteinase K (Fermentas) treatment, immunoprecipitated DNA was purified using the QIAquick PCR purification kit (Qiagen) and analyzed by quantitative real-time PCR (primer sequences are listed in Table S3) and relative occupancies were normalized to input DNA (fold difference= $2^{-Ct\text{-}sample\text{-}Ct\text{-}input}$). To control for non-specific binding, a 82 base pair fragment in a gene desert in chromosome 6 (ActiveMotif) was used.

RNA sequencing and analysis

Total RNA was extracted using TRIzol (Life technologies) and cDNA libraries were prepared using the Stranded mRNA-Seq Kit (Kapa Biosystems). Briefly, poly-A tailed RNA was purified using paramagnetic oligo-dT beads from 200 nanograms of total RNA, with a RNA Integrity Number above 7.5 as determined by the Agilent Bioanalyzer. The purified RNA was chemically fragmented and cDNA was synthesised using random primers (Kapa Biosystems). Adapter-ligated DNA library was amplified with 12 cycles of PCR and library fragment was estimated using the Agilent TapeStation 2200.Library concentration was determined using the Qubit DNA HS assay (Life Technologies). Libraries were sequenced on an Illumina NextSeq 500, NCS v2.1.2 (Illumina) with a 43bp paired end protocol. Basecalling was done using standard Illumina parameters (RTA 2.4.11). Sequencing and pipeline analysis was performed by UCL Genomics (London, UK). Reads were demulitplexed using Illumina's bcl2fastq v2.17 and aligned using STAR v2.5.0b to the mouse GRCm38/mm10 reference sequence. Transcript abundance was estimated using Illumina's RnaReadCounter tool and differential expression analysis performed with DESeq2, which uses the Benjamin-Hochberg method for multiple testing correction. Pathway enrichment analysis was performed with the Gene Set Enrichment Analysis (GSEA) software's pre-ranked module (Mootha et al., 2003; Subramanian et al., 2005). Top regulated genes were confirmed by qPCR on a separate set of liver samples from HFHC-fed mice. Heatmaps were created using raw gene count values with the MultiExperiment Viewer (MeV) software (Howe et al., 2011).

Statistical analysis.

Data is presented as mean ± SEM. Differences were considered significant at $p < 0.05$ by a two-tailed Student t-test. For multiple comparisons, significance was assessed by single variance ANOVA followed by Student's T-test. The *F*-statistic ($df_{between}=3$, $df_{within}=15$) and the *P* value for the significant main effect are shown.

REFERENCES

Aguilar-olivos, N.E., Carrillo-córdova, D., Oria-hernández, J., Sánchez-valle, V., Ponciano-rodríguez, G., and Ramírez-jaramillo, M. (2015). The nuclear receptor FXR , but not LXR , up-regulates bile acid transporter expression in non-alcoholic fatty liver disease. Ann. Hepatol. Off. J. Mex. Assoc. Hepatol. *14*, 487–493.

Ahn, S.B., Jang, K., Jun, D.W., Lee, B.H., and Shin, K.J. (2014). Expression of liver X receptor correlates with intrahepatic inflammation and fibrosis in patients with nonalcoholic fatty liver disease. Dig. Dis. Sci. *59*, 2975–2982.

Beaven, S.W., Wroblewski, K., Wang, J., Hong, C., Bensinger, S., Tsukamoto, H., and Tontonoz, P. (2011). Liver X Receptor Signaling Is a Determinant of Stellate Cell Activation and Susceptibility to Fibrotic Liver Disease. Gastroenterology *140*, 1052–1062.

Becares, N., Gage, M.C., and Pineda-Torra, I. (2016). Posttranslational Modifications of Lipid-Activated Nuclear Receptors: Focus on Metabolism. Endocrinology *158*, 213–225.
Bellentani, S., Scaglioni, F., Marino, M., and Bedogni, G. (2010). Epidemiology of Non-Alcoholic Fatty Liver Disease. Dig. Dis. *28*, 155–161.

Bellezza, I., Roberti, R., Gatticchi, L., Del Sordo, R., Rambotti, M.G., Marchetti, M.C., Sidoni, A., and Minelli, A. (2013). A Novel Role for Tm7sf2 Gene in Regulating TNFα Expression. PLoS One *8*, e68017.

Boergesen, M., Pedersen, T.A., Gross, B., van Heeringen, S.J., Hagenbeek, D., Bindesboll, C., Caron, S., Lalloyer, F., Steffensen, K.R., Nebb, H.I., et al. (2012). Genome-Wide Profiling of Liver X Receptor, Retinoid X Receptor, and Peroxisome Proliferator-Activated Receptor in Mouse Liver Reveals Extensive Sharing of Binding Sites. Mol. Cell. Biol. *32*, 852–867.

Bonamassa, B., and Moschetta, A. (2013). Atherosclerosis: lessons from LXR and the intestine. Trends Endocrinol. Metab. *24*, 120–128.

Cha, J.-Y., and Repa, J.J. (2007). The liver X receptor (LXR) and hepatic lipogenesis. The carbohydrate-response element-binding protein is a target gene of LXR. J. Biol. Chem. *282*, 743–751.

Chen, M., Bradley, M.N., Beaven, S.W., and Tontonoz, P. (2006). Phosphorylation of the liver X receptors. FEBS Lett. *580*, 4835–4841.

Cho, K., Chung, J.Y., Cho, S.K., Shin, H.-W., Jang, I.-J., Park, J.-W., Yu, K.-S., and Cho, J.-Y. (2015). Antihyperglycemic mechanism of metformin occurs via the AMPK/LXRα/POMC pathway. Sci. Rep. *5*, 8145.

Dara, L., Ji, C., and Kaplowitz, N. (2011). The contribution of endoplasmic reticulum stress to liver

diseases. Hepatology *53*, 1752–1763.

Devries-Seimon, T., Li, Y., Yao, P.M., Stone, E., Wang, Y., Davis, R.J., Flavell, R., and Tabas, I. (2005). Cholesterol-induced macrophage apoptosis requires ER stress pathways and engagement of the type A scavenger receptor. J. Cell Biol. *171*, 61–73.

Duda, R.O., and Hart, P.E. (1972). Use of the Hough transformation to detect lines and curves in pictures. Commun. ACM *15*, 11–15.

EASL, EASD, and EASO (2016). EASL-EASD-EASO Clinical Practice Guidelines for the management of non-alcoholic fatty liver disease.

Fan, R., Toubal, A., Goñi, S., Drareni, K., Huang, Z., Alzaid, F., Ballaire, R., Ancel, P., Liang, N., Damdimopoulos, A., et al. (2016). Loss of the co-repressor GPS2 sensitizes macrophage activation upon metabolic stress induced by obesity and type 2 diabetes. Nat. Med. *22*, 780–791.

Fungwe, T. V, Fox, J.E., Cagen, L.M., Wilcox, H.G., and Heimberg, M. (1994). Stimulation of fatty acid biosynthesis by dietary cholesterol and of cholesterol synthesis by dietary fatty acid. J Lipid Res. *35*, 311–318.

Gaggini, M., Morelli, M., Buzzigoli, E., DeFronzo, R., Bugianesi, E., and Gastaldelli, A. (2013). Non-Alcoholic Fatty Liver Disease (NAFLD) and Its Connection with Insulin Resistance, Dyslipidemia, Atherosclerosis and Coronary Heart Disease. Nutrients *5*, 1544–1560.

Grefhorst, A., Elzinga, B.M., Voshol, P.J., Plösch, T., Kok, T., Bloks, V.W., Van Der Sluijs, F.H., Havekes, L.M., Romijn, J.A., Verkade, H.J., et al. (2002). Stimulation of lipogenesis by pharmacological activation of the liver X receptor leads to production of large, triglyceride-rich very low density lipoprotein particles. J. Biol. Chem. *277*, 34182–34190.

Griffett, K., Solt, L., El-Gendy, B.-D., Kamenecka, T., and Burris, T. (2013). A liver-selective LXR inverse agonist that suppresses hepatic steatosis. ACS Chem. Biol. *8*, 559–567.

Griffett, K., Welch, R.D., Flaveny, C. a., Kolar, G.R., Neuschwander-Tetri, B. a., and Burris, T.P. (2015). The LXR inverse agonist SR9238 suppresses fibrosis in a model of non-alcoholic steatohepatitis. Mol. Metab. *4*, 353–357.

Hamilton, J.P., Koganti, L., Muchenditsi, A., Pendyala, V.S., Huso, D., Hankin, J., Murphy, R.C., Huster, D., Merle, U., Mangels, C., et al. (2016). Activation of liver X receptor/retinoid X receptor

pathway ameliorates liver disease in Atp7B(-/-) (Wilson disease) mice. Hepatology *63*, 1828–1841.

Howe, E.A., Sinha, R., Schlauch, D., and Quackenbush, J. (2011). RNA-Seq analysis in MeV. Bioinformatics *27*, 3209–3210.

Hwahng, S.H., Ki, S.H., Bae, E.J., Kim, H.E., and Kim, S.G. (2009). Role of adenosine monophosphate-activated protein kinase-p70 ribosomal S6 kinase-1 pathway in repression of liver X receptor-alpha-dependent lipogenic gene induction and hepatic steatosis by a novel class of dithiolethiones. Hepatology *49*, 1913–1925.

Ikegami, T., Hyogo, H., Honda, A., Miyazaki, T., Tokushige, K., Hashimoto, E., Inui, K., Matsuzaki, Y., and Tazuma, S. (2012). Increased serum liver X receptor ligand oxysterols in patients with non-alcoholic fatty liver disease. J. Gastroenterol. *47*, 1257–1266.

Jakobsson, T., Venteclef, N., Toresson, G., Damdimopoulos, A.E., Ehrlund, A., Lou, X., Sanyal, S., Steffensen, K.R., Gustafsson, J.-Å., and Treuter, E. (2009). GPS2 Is Required for Cholesterol Efflux by Triggering Histone Demethylation, LXR Recruitment, and Coregulator Assembly at the ABCG1 Locus.

Janowski, B.A., Willy, P.J., Devi, T.R., Falck, J.R., and Mangelsdorf, D.J. (1996). An oxysterol signalling pathway mediated by the nuclear receptor LXR alpha. Nature *383*, 728–731.
Jones, R.D., Taylor, A.M., Tong, E.Y., and Repa, J.J. (2013). Carboxylesterases are uniquely expressed among tissues and regulated by nuclear hormone receptors in the mouse. Drug Metab. Dispos. *41*, 40–49.

Joseph, S.B., Laffitte, B.A., Patel, P.H., Watson, M.A., Matsukuma, K.E., Walczak, R., Collins, J.L., Osborne, T.F., and Tontonoz, P. (2002). Direct and indirect mechanisms for regulation of fatty acid synthase gene expression by liver X receptors. J. Biol. Chem. *277*, 11019–11025.

Kalaany, N.Y., Gauthier, K.C., Zavacki, A.M., Mammen, P.P.A., Kitazume, T., Peterson, J.A., Horton, J.D., Garry, D.J., Bianco, A.C., and Mangelsdorf, D.J. (2005). LXRs regulate the balance between fat storage and oxidation. Cell Metab. *1*, 231–244.

Kanta, J. (2016). Elastin in the Liver. Front. Physiol. *7*, 491.

Kleiner, D.E., Brunt, E.M., Van Natta, M., Behling, C., Contos, M.J., Cummings, O.W., Ferrell, L.D., Liu, Y.C., Torbenson, M.S., Unalp-Arida, A., et al. (2005). Design and validation of a histological scoring system for nonalcoholic fatty liver disease. Hepatology *41*, 1313–1321.

Kockx, M., Dinnes, D.L., Huang, K.-Y., Sharpe, L.J., Jessup, W., Brown, A.J., and Kritharides, L. (2012). Cholesterol accumulation inhibits ER to Golgi transport and protein secretion: studies of apolipoprotein E and VSVGt. Biochem. J. *447*, 51–60.

Koentgen, F., Suess, G., and Naf, D. (2010). Engineering the Mouse Genome to Model Human Disease for Drug Discovery. In Methods in Molecular Biology (Clifton, N.J.), pp. 55–77.

Laffitte, B.A., Repa, J.J., Joseph, S.B., Wilpitz, D.C., Kast, H.R., Mangelsdorf, D.J., and Tontonoz, P. (2001). LXRs control lipid-inducible expression of the apolipoprotein E gene in macrophages and adipocytes. Proc. Natl. Acad. Sci. U. S. A. *98*, 507–512.

Lebeaupin, C., Proics, E., de Bieville, C.H.D., Rousseau, D., Bonnafous, S., Patouraux, S., Adam, G., Lavallard, V.J., Rovere, C., Le Thuc, O., et al. (2015). ER stress induces NLRP3 inflammasome activation and hepatocyte death. Cell Death Dis. *6*, e1879.

Lehmann, J.M., Kliewer, S.A., Moore, L.B., Smith-Oliver, T.A., Oliver, B.B., Su, J.L., Sundseth, S.S., Winegar, D.A., Blanchard, D.E., Spencer, T.A., et al. (1997). Activation of the nuclear receptor LXR by oxysterols defines a new hormone response pathway. J. Biol. Chem. *272*, 3137–3140.

Li, J., Wang, Y., Matye, D.J., Chavan, H., Krishnamurthy, P., Li, F., and Li, T. (2017). Sortilin 1 Modulates Hepatic Cholesterol Lipotoxicity in Mice via Functional Interaction with Liver Carboxylesterase 1. J. Biol. Chem. *292*, 146–160.

Li, X., Zhang, S., Blander, G., Tse, J.G., Krieger, M., and Guarente, L. (2007). SIRT1 Deacetylates and Positively Regulates the Nuclear Receptor LXR. Mol. Cell *28*, 91–106.

Liang, W., Menke, A.L., Driessen, A., Koek, G.H., Lindeman, J.H., Stoop, R., Havekes, L.M., Kleemann., R., and Van Den Hoek, A.M. (2014). Establishment of a general NAFLD scoring system for rodent models and comparison to human liver pathology. PLoS One *9*, 1–17.

Lima-Cabello, E., García-Mediavilla, M.V., Miquilena-Colina, M.E., Vargas-Castrillón, J., Lozano-Rodríguez, T., Fernández-Bermejo, M., Olcoz, J.L., González-Gallego, J., García-Monzón, C., and Sánchez-Campos, S. (2011). Enhanced expression of pro-inflammatory mediators and liver X-receptor-regulated lipogenic genes in non-alcoholic fatty liver disease and hepatitis C. Clin. Sci. (Lond). *120*, 239–250.

Liu, S.B., Ikenaga, N., Peng, Z.-W., Sverdlov, D.Y., Greenstein, A., Smith, V., Schuppan, D., and Popov, Y. (2016). Lysyl oxidase activity contributes to collagen stabilization during liver fibrosis progression and limits spontaneous fibrosis reversal in mice. FASEB J. *30*, 1599–1609.

Marí, M., Caballero, F., Colell, A., Morales, A., Caballeria, J., Fernandez, A., Enrich, C., Fernandez-Checa, J.C., and García-Ruiz, C. (2006). Mitochondrial free cholesterol loading sensitizes to TNF-and Fas-mediated steatohepatitis. Cell Metab. *4*, 185–198.

Mootha, V.K., Lindgren, C.M., Eriksson, K.-F., Subramanian, A., Sihag, S., Lehar, J., Puigserver, P., Carlsson, E., Ridderstråle, M., Laurila, E., et al. (2003). PGC-1α-responsive genes involved in oxidative phosphorylation are coordinately downregulated in human diabetes. Nat. Genet. *34*, 267–273.

Moylan, C.A., Pang, H., Dellinger, A., Suzuki, A., Garrett, M.E., Guy, C.D., Murphy, S.K., Ashley-Koch, A.E., Choi, S.S., Michelotti, G.A., et al. (2014). Hepatic gene expression profiles differentiate presymptomatic patients with mild versus severe nonalcoholic fatty liver disease. Hepatology *59*, 471–482.

Musso, G., Gambino, R., Cassader, M., and Pagano, G. (2011). Meta-analysis: Natural history of non-alcoholic fatty liver disease (NAFLD) and diagnostic accuracy of non-invasive tests for liver disease severity. Ann. Med. *43*, 617–649.

Pawlak, M., Lefebvre, P., and Staels, B. (2012). General molecular biology and architecture of nuclear receptors. Curr. Top. Med. Chem. *12*, 486–504.

Peet, D.J., Turley, S.D., Ma, W., Janowski, B.A., Lobaccaro, J.M.A., Hammer, R.E., and Mangelsdorf, D.J. (1998). Cholesterol and bile acid metabolism are impaired in mice lacking the nuclear oxysterol receptor LXRalpha. Cell *93*, 693–704.

Pehkonen, P., Welter-Stahl, L., Diwo, J., Ryynänen, J., Wienecke-Baldacchino, A., Heikkinen, S., Treuter, E., Steffensen, K.R., and Carlberg, C. (2012). Genome-wide landscape of liver X receptor chromatin binding and gene regulation in human macrophages. BMC Genomics *13*, 50.

Perissi, V., Aggarwal, A., Glass, C.K., Rose, D.W., and Rosenfeld, M.G. (2004). A corepressor/coactivator exchange complex required for transcriptional activation by nuclear receptors and other regulated transcription factors. Cell *116*, 511–526.

Pourcet, B., Gage, M.C., León, T.E., Waddington, K.E., Pello, O.M., Steffensen, K.R., Castrillo, A.,

Valledor, A.F., and Pineda-Torra, I. (2016). The nuclear receptor LXR modulates interleukin-18 levels in macrophages through multiple mechanisms. Sci. Rep. *6*, 25481.

Quiroga, A.D., Li, L., Trötzmüller, M., Nelson, R., Proctor, S.D., Köfeler, H., and Lehner, R. (2012). Deficiency of carboxylesterase 1/esterase-x results in obesity, hepatic steatosis, and hyperlipidemia. Hepatology *56*, 2188–2198.

Repa, J.J., Liang, G., Ou, J., Bashmakov, Y., Lobaccaro, J.M.A., Shimomura, I., Shan, B., Brown, M.S., Goldstein, J.L., and Mangelsdorf, D.J. (2000a). Regulation of mouse sterol regulatory element-binding protein-1c gene (SREBP-1c) by oxysterol receptors, LXRalpha and LXRbeta. Genes Dev. *14*, 2819–2830.

Repa, J.J., Turley, S.D., Lobaccaro, J.A., Medina, J., Li, L., Lustig, K., Shan, B., Heyman, R.A., Dietschy, J.M., and Mangelsdorf, D.J. (2000b). Regulation of absorption and ABC1-mediated efflux of cholesterol by RXR heterodimers. Science *289*, 1524–1529.

Repa, J.J., Berge, K.E., Pomajzl, C., Richardson, J.A., Hobbs, H., and Mangelsdorf, D.J. (2002). Regulation of ATP-binding cassette sterol transporters ABCG5 and ABCG8 by the liver X receptors alpha and beta. J. Biol. Chem. *277*, 18793–18800.

Roberg-Larsen, H., Lund, K., Vehus, T., Solberg, N., Vesterdal, C., Misaghian, D., Olsen, P.A., Krauss, S., Wilson, S.R., and Lundanes, E. (2014). Highly automated nano-LC/MS-based approach for thousand cell-scale quantification of side chain-hydroxylated oxysterols. J. Lipid Res. *55*, 1531–1536.

Roberg-Larsen, H., Lund, K., Seterdal, K.E., Solheim, S., Vehus, T., Solberg, N., Krauss, S., Lundanes, E., and Wilson, S.R. (2016). Mass spectrometric detection of 27-hydroxycholesterol in breast cancer exosomes. J. Steroid Biochem. Mol. Biol.

Sanyal, A.J. (2005). Mechanisms of Disease: pathogenesis of nonalcoholic fatty liver disease. Nat. Clin. Pract. Gastroenterol. Hepatol. *2*, 46–53.

Savard, C., Tartaglione, E. V., Kuver, R., Haigh, W.G., Farrell, G.C., Subramanian, S., Chait, A., Yeh, M.M., Quinn, L.S., and Ioannou, G.N. (2013). Synergistic interaction of dietary cholesterol and dietary fat in inducing experimental steatohepatitis. Hepatology *57*, 81–92.

Schultz, J.R., Tu, H., Luk, A., Repa, J.J., Medina, J.C., Li, L., Schwendner, S., Wang, S., Thoolen, M., Mangelsdorf, D.J., et al. (2000). Role of LXRs in control of lipogenesis. Genes Dev. *14*, 2831–

2838.

Semba, T., Nishimura, M., Nishimura, S., Ohara, O., Ishige, T., Ohno, S., Nonaka, K., Sogawa, K., Satoh, M., Sawai, S., et al. (2013). The FLS (Fatty liver Shionogi) mouse reveals local expressions of lipocalin-2, CXCL1 and CXCL9 in the liver with non-alcoholic steatohepatitis. BMC Gastroenterol. *13*, 120.

Shrestha, E., Hussein, M.A., Savas, J.N., Ouimet, M., Barrett, T.J., Leone, S., Yates, J.R., Moore, K.J., Fisher, E.A., and Garabedian, M.J. (2016). Poly(ADP-ribose) Polymerase 1 Represses Liver X Receptor-mediated ABCA1 Expression and Cholesterol Efflux in Macrophages. J. Biol. Chem. *291*, 11172–11184.

Steffensen, K.R., Jakobsson, T., and Gustafsson, J.-Å. (2013). Targeting liver X receptors in inflammation. Expert Opin. Ther. Targets *17*, 977–990.

Subramanian, A., Tamayo, P., Mootha, V.K., Mukherjee, S., Ebert, B.L., Gillette, M.A., Paulovich, A., Pomeroy, S.L., Golub, T.R., Lander, E.S., et al. (2005). Gene set enrichment analysis: a knowledge-based approach for interpreting genome-wide expression profiles. Proc. Natl. Acad. Sci. U. S. A. *102*, 15545–15550.

Syn, W.-K., Choi, S.S., Liaskou, E., Karaca, G.F., Agboola, K.M., Oo, Y.H., Mi, Z., Pereira, T.A., Zdanowicz, M., Malladi, P., et al. (2011). Osteopontin is induced by hedgehog pathway activation and promotes fibrosis progression in nonalcoholic steatohepatitis. Hepatology *53*, 106–115.

Takeuchi, T., Nomura, T., Tsujita, M., Suzuki, M., Fuse, T., Mori, H., and Mishina, M. (2002). Flp recombinase transgenic mice of C57BL/6 strain for conditional gene targeting. Biochem. Biophys. Res. Commun. *293*, 953–957.

Tall, A.R., and Yvan-Charvet, L. (2015). Cholesterol, inflammation and innate immunity. Nat. Rev. Immunol. *15*, 104–116.

Thoma, C., Day, C.P., and Trenell, M.I. (2012). Lifestyle interventions for the treatment of non-alcoholic fatty liver disease in adults: A systematic review. J. Hepatol. *56*, 255–266.

Tomita, K., Teratani, T., Suzuki, T., Shimizu, M., Sato, H., Narimatsu, K., Okada, Y., Kurihara, C., Irie, R., Yokoyama, H., et al. (2014). Free cholesterol accumulation in hepatic stellate cells: Mechanism of liver fibrosis aggravation in nonalcoholic steatohepatitis in mice. Hepatology *59*, 154–169.

Torra, I.P., Ismaili, N., Feig, J.E., Xu, C.-F., Cavasotto, C., Pancratov, R., Rogatsky, I., Neubert, T.A., Fisher, E.A., and Garabedian, M.J. (2008). Phosphorylation of liver X receptor alpha selectively regulates target gene expression in macrophages. Mol. Cell. Biol. *28*, 2626–2636.

Torra, I.P., Staverosky, J.A., Ha, S., Logan, S.K., and Garabedian, M.J. (2009). Development of Phosphorylation Site-Specific Antibodies to Nuclear Receptors. In Methods in Molecular Biology (Clifton, N.J.), pp. 221–235.

Uppal, H., Saini, S.P.S., Moschetta, A., Mu, Y., Zhou, J., Gong, H., Zhai, Y., Ren, S., Michalopoulos, G.K., Mangelsdorf, D.J., et al. (2007). Activation of LXRs prevents bile acid toxicity and cholestasis in female mice. Hepatology *45*, 422–432.

Venkateswaran, A., Repa, J.J., Lobaccaro, J.M.A., Bronson, A., Mangelsdorf, D.J., and Edwards, P.A. (2000). Human white/murine ABC8 mRNA levels are highly induced in lipid-loaded macrophages. A transcriptional role for specific oxysterols. J. Biol. Chem. *275*, 14700–14707.

Wu, C., Hussein, M., Shrestha, E., Leone, S., Aiyegbo, M.S., Lambert, W.M., Pourcet, B., Cardozo, T., Gustaffson, J.-A., Fisher, E.A., et al. (2015). Modulation of macrophage gene expression via LXRα serine 198 phosphorylation. Mol. Cell. Biol. *35*, 2024–2034.

Wu, J.E., Basso, F., Shamburek, R.D., Amar, M.J.A., Vaisman, B., Szakacs, G., Joyce, C., Tansey, T., Freeman, L., Paigen, B.J., et al. (2004). Hepatic ABCG5 and ABCG8 overexpression increases hepatobiliary sterol transport but does not alter aortic atherosclerosis in transgenic mice. J. Biol. Chem. *279*, 22913–22925.

Xu, J., Xu, Y., Li, Y., Jadhav, K., You, M., Yin, L., Zhang, Y., Starr, S.P., Raines, D., Gao, B., et al. (2016). Carboxylesterase 1 Is Regulated by Hepatocyte Nuclear Factor 4α and Protects Against Alcohol- and MCD diet-induced Liver Injury. Sci. Rep. *6*, 24277.

Yamamoto T, Shimano H, Inoue N, Nakagawa Y, Matsuzaka T, Takahashi A, Yahagi N, Sone H, Suzuki H, Toyoshima H, Y.N. (2007). Protein Kinase A Suppresses Sterol Regulatory Element-binding Protein-1C Expression via Phosphorylation of Liver X Receptor in the Liver. J Biol Chem. *282*, 11687–11695.

Zhang, Y., Breevoort, S.R., Angdisen, J., Fu, M., Schmidt, D.R., Holmstrom, S.R., Kliewer, S.A., Mangelsdorf, D.J., and Schulman, I.G. (2012). Liver LXRα expression is crucial for whole body cholesterol homeostasis and reverse cholesterol transport in mice. J. Clin. Invest. *122*, 1688–1699.

Zhao, B., Natarajan, R., and Ghosh, S. (2005). Human liver cholesteryl ester hydrolase: cloning, molecular characterization, and role in cellular cholesterol homeostasis. Physiol. Genomics *23*, 304–310.

Znoyko, I., Sohara, N., Spicer, S.S., Trojanowska, M., and Reuben, A. (2005). Expression of oncostatin M and its receptors in normal and cirrhotic human liver. J. Hepatol. *43*, 893–900.

Figure Legends

Figure 1. LXRα-S196A mice develop enhanced steatosis on a high cholesterol diet.

A) LXRα phosphorylation at Ser196 analysed by LXRα/β immunoprecipitation of liver homogenates and immunoblotting with a phospho-S196-LXRα specific antibody. Global LXRα expression was assessed.

B) Hepatic non-esterified fatty acids (NEFAs) or triglyceride (TGs) in mice fed a HFHC diet (n=6/group) normalized to liver protein levels.

C) Kleiner's scores for steatosis (0-3) of liver sections (n≥5/group).

D) Representative images of Haematoxylin and Eosin (H&E) stained liver sections from mice fed chow or HFHC diet. 400x magnifications. Scale bar at 50 μM.

E) Distribution of lipid droplets by area in H&E -stained liver sections (n=6/group). Area distribution was compared by chi-square test for trend (p= 0.0003).

F) Hepatic gene expression in mice fed a HFHC diet (n=6/group). Normalized data are shown relative to WT, set as 1. Data are means ± SEM. *p<0.05, **p<0.005 or ***p<0.001 relative to WT.

Figure 2. S196A-LXRα alleviates diet-induced hepatic inflammation and fibrosis

A) Kleiner's Scores for lobular inflammation (0-3) from liver sections of mice (n=6/group).

B) Representative images of Picrosirius Red stained liver sections (left). 200x magnification. Scale bar at 100 μM. Quantification of stained areas by Image J (n=6/group) (right). Values are the average positively-stained percentage of area of interest.

C) Hepatic gene expression (n=6/group). Normalized data are shown relative to WT.

D) Hepatic gene expression in mice fed chow (n=4/group) or HFHC diet (n=6/group). Normalized data shown relative to WT chow group. *p<0.05, **p<0.005, ***p< 0.0005, relative to WT chow.

E) Hepatic gene expression (n=6/group). Values shown normalized to cyclophilin and relative to WT.

Data are means ± SEM. *p<0.05, **p<0.005 relative to WT.

Figure 3. LXR phosphorylation deficient mice show reduced cholesterol levels in response to a HFHC diet.

A) Plasma total cholesterol levels in mice fed a chow (n=4/group) or a HFHC diet (n≥5/group).

B) Hepatic total cholesterol levels in mice fed a HFHC diet (n=6/group). Values shown normalized to protein levels in tissue homogenates.

C) Hepatic gene expression in fed a HFHC diet (n=6/group). Normalized data shown relative to WT.

D-E) Hepatic gene expression in mice fed chow (n=4) or a HFHC diet (n=6). Normalized data shown relative to WT chow group

F) Quantification of free oxysterols in plasma of mice fed a HFHC diet (n=6/group).

Data are means ± SEM. *p<0.05, **p<0.005, ***p<0.0005, ****p<0.00005 relative to WT. ##p<0.005, 4 vs 6 weeks.

Figure 4. Changes in LXRα phosphorylation reprogram hepatic gene expression.

A) Volcano plot of $\log_2$ ratio vs p-value of differentially expressed genes comparing S196A and WT livers (n=3). Blue line indicates adjusted p-value threshold of 0.04 (Wald Test for logistic regression).

B) GSEA analysis showing enriched pathways in S196A livers with a nominal p<0.5 (100 permutations) derived from HALLMARK gene sets.

C-E) Heatmaps representing hepatic RNAseq raw gene counts (n=3/group). C) Fatty acid and triglyceride metabolism, D) Fibrosis and E) Human NAFLD signature genes.

F) Hepatic gene expression by qPCR of top 10 induced genes from the RNAseq analysis on experimentally-independent WT and S196A livers (n=6/group). Normalized data shown relative to WT.

G-I) LXR, RXR and TBLR1 occupancy at Ces1f (G) and Cyp2c69 (H) DR4 and Srebp-1c LXRE (I) or a region within in a gene desert (Neg S) in livers of mice fed HFHC for 6 weeks (n≥3/group). Results shown normalized to input and relative to WT.

F) Diagram depicting how the S196A-LXRα induces expression of novel phosphorylation-sensitive genes in a cholesterol-rich environment.

Data represents mean ± SEM. #p=0.05, *p<0.05, **p<0.005 or ***p<0.005 relative to WT.

Acknowledgements

We are grateful to Prof Edward Fisher (New York University School of Medicine) and Dr James Thorne (University of Leeds) for insightful discussions. This work was supported by a Medical Research Council New Investigator Grant G0801278 (IPT), British Heart Foundation Project Grant PG/13/10/30000 (IPT), UCL Grand Challenges PhD Studentship (NB, IPT), Swedish Research Council (VR2016-01743) (ET), Center for Innovative Medicine at Karolinska Institutet (ET) and University of Oslo DIATECH@UiO strategic research initiative (HRL).

Author Contributions

N.B. performed most of the experiments, data analysis and prepared figures. M.G. helped to establish mouse colonies, performed experiments and data interpretation. L.M.G. helped with qPCR and analysed data. B.P. and O.M.P. helped establish initial floxed and global S196A mouse colonies. T.V.L scored liver sections. S.G., N.L. and E.T. provided unpublished ChIPseq data in liver. C.P. and V.D. developed software to analyse lipid droplets. H.R-L. performed oxysterol analyses. K.R.S. and K.R. provided materials. M.J.G. provided materials and shared data and E.S. performed proteomic analyses. K.R., M.G and E.T. helped with data interpretation. N.B. and I.P.T

designed experiments, interpreted data and wrote the manuscript. I.P.T. conceived the study, secured funding and supervised all aspects of the work.

Figure 1

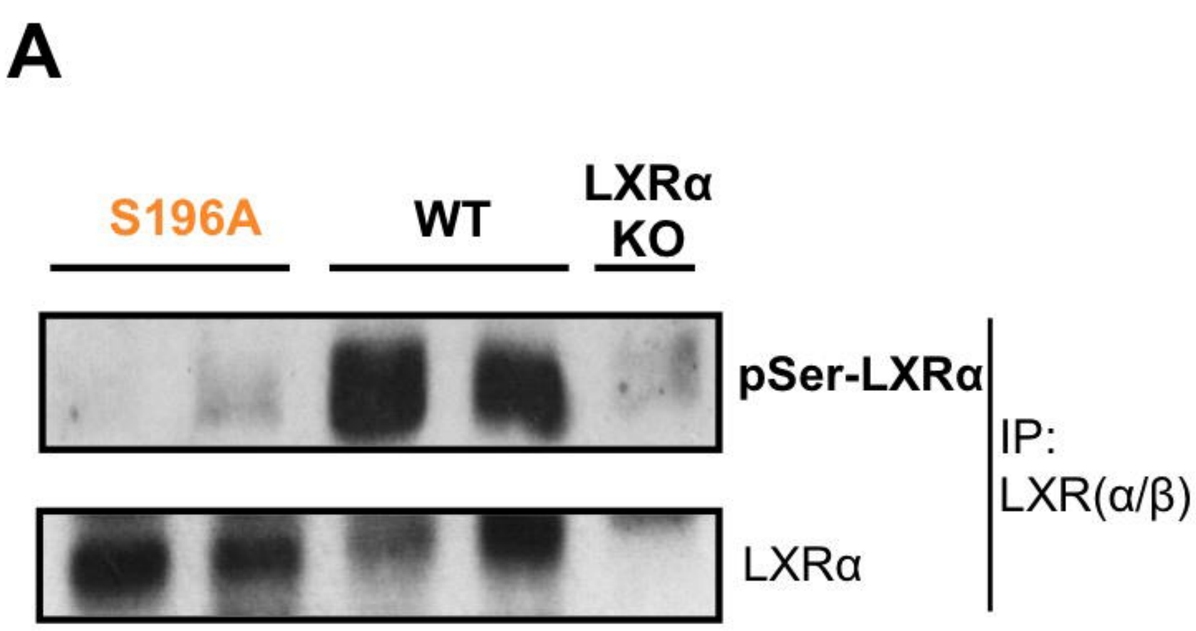

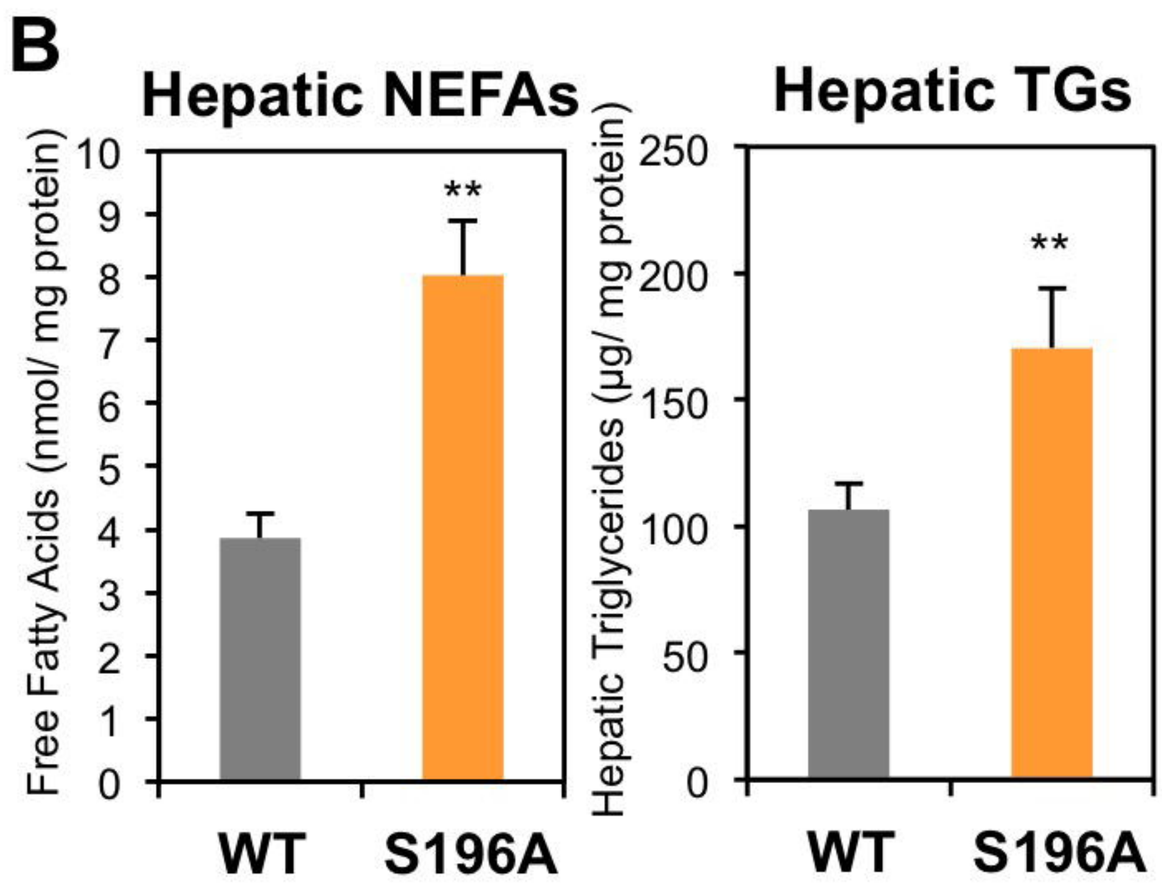

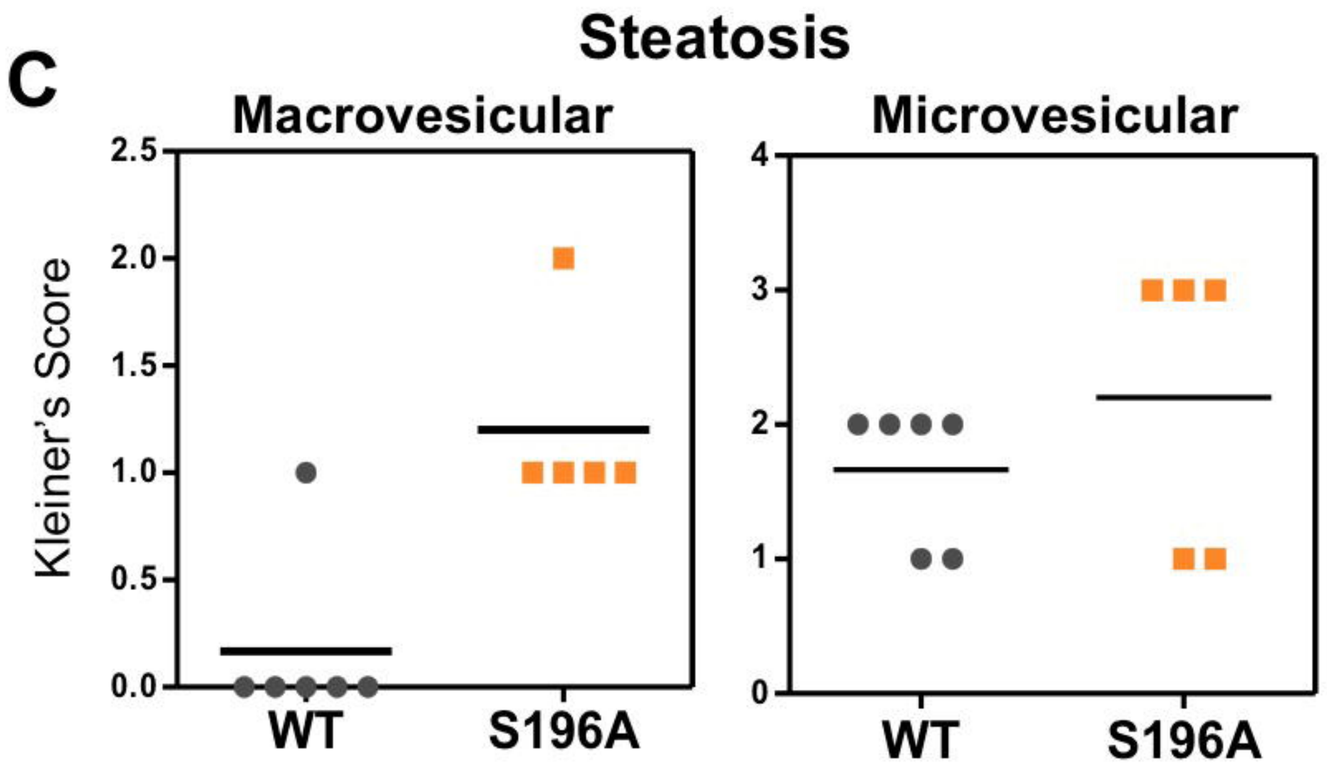

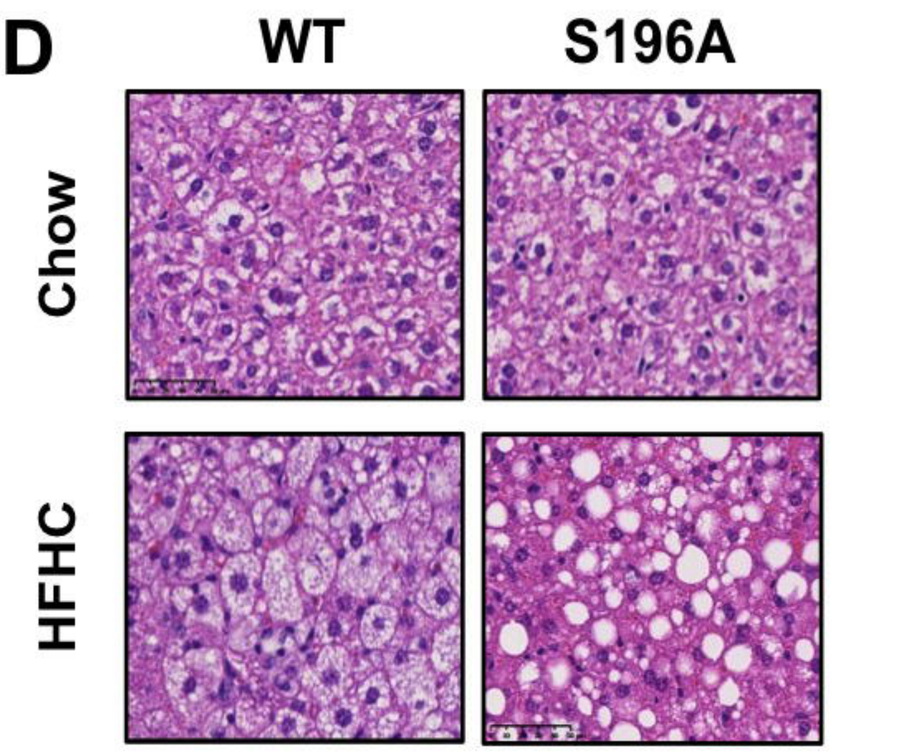

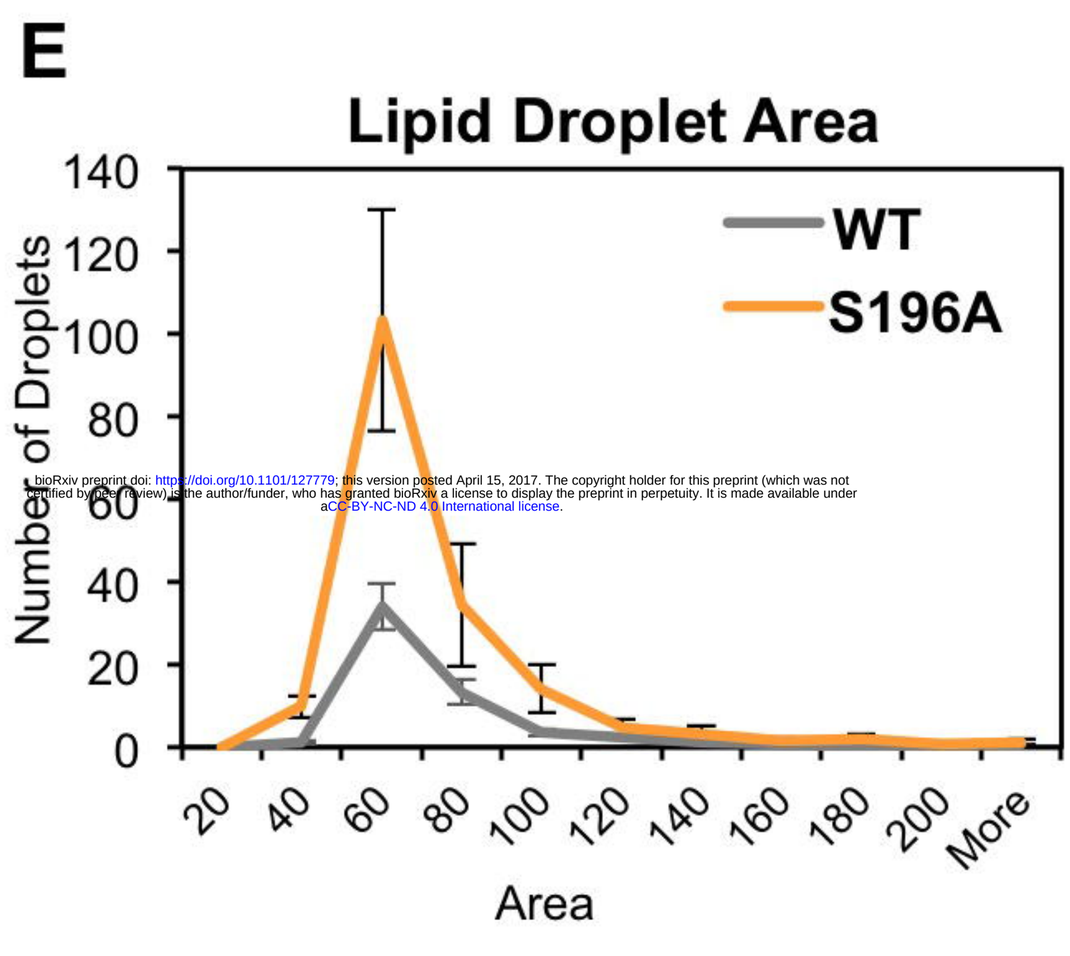

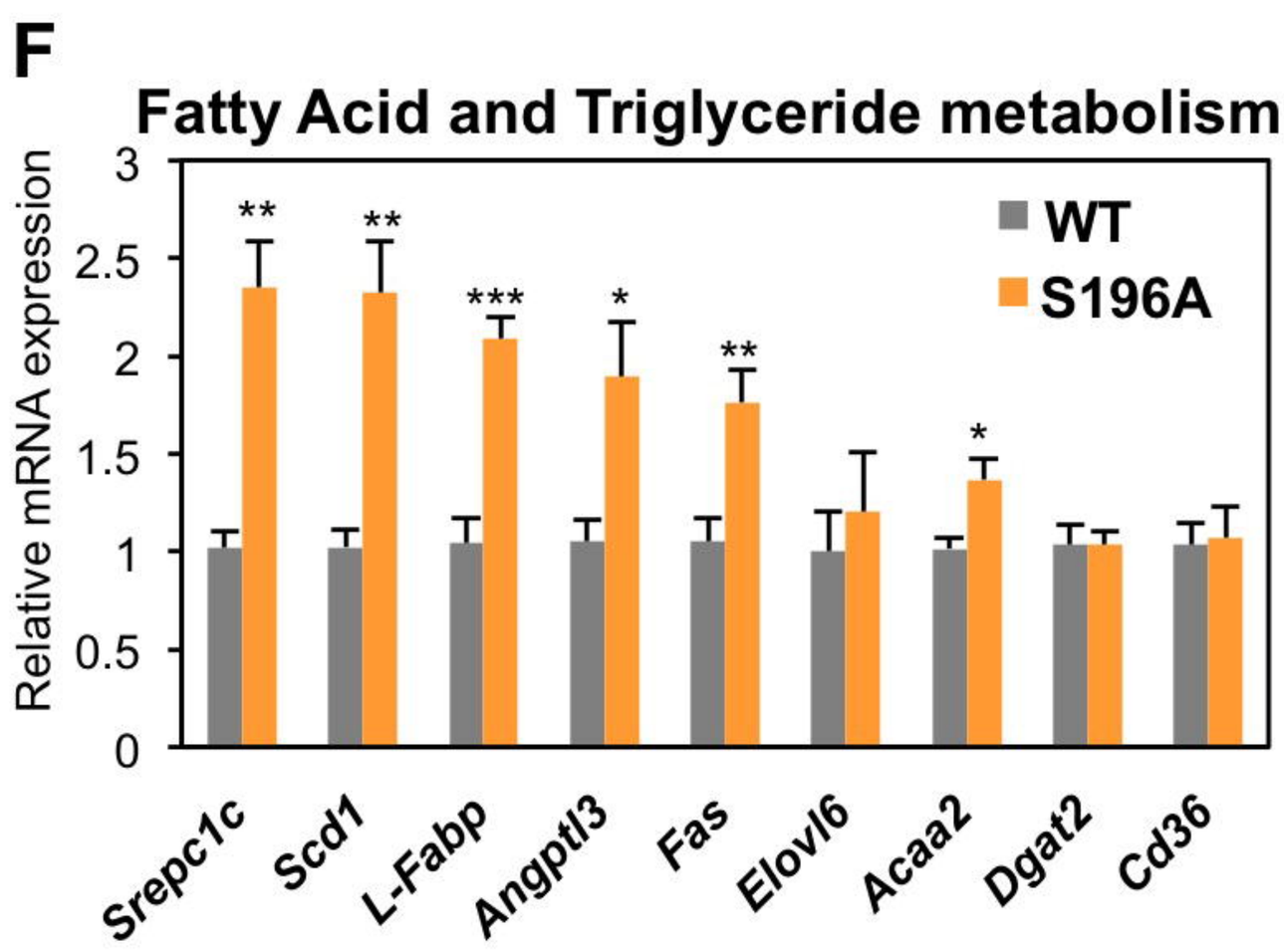

Figure 2

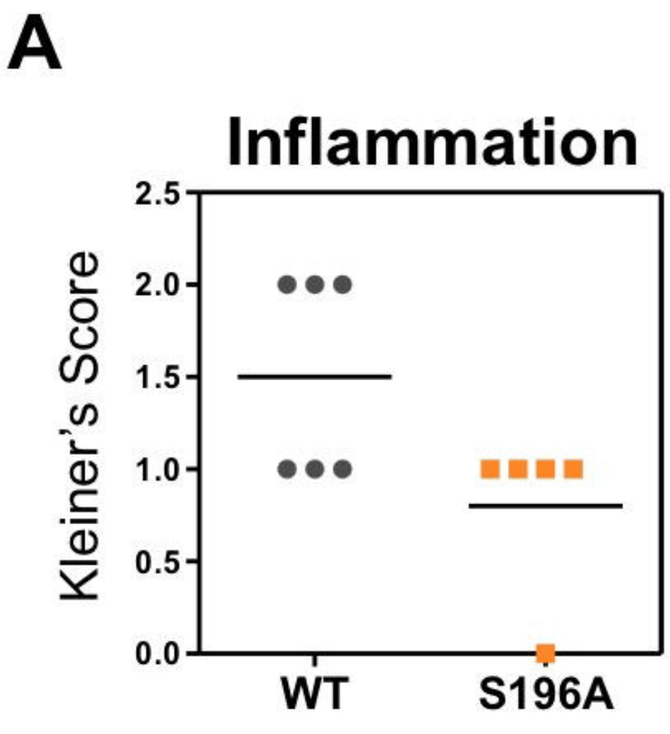

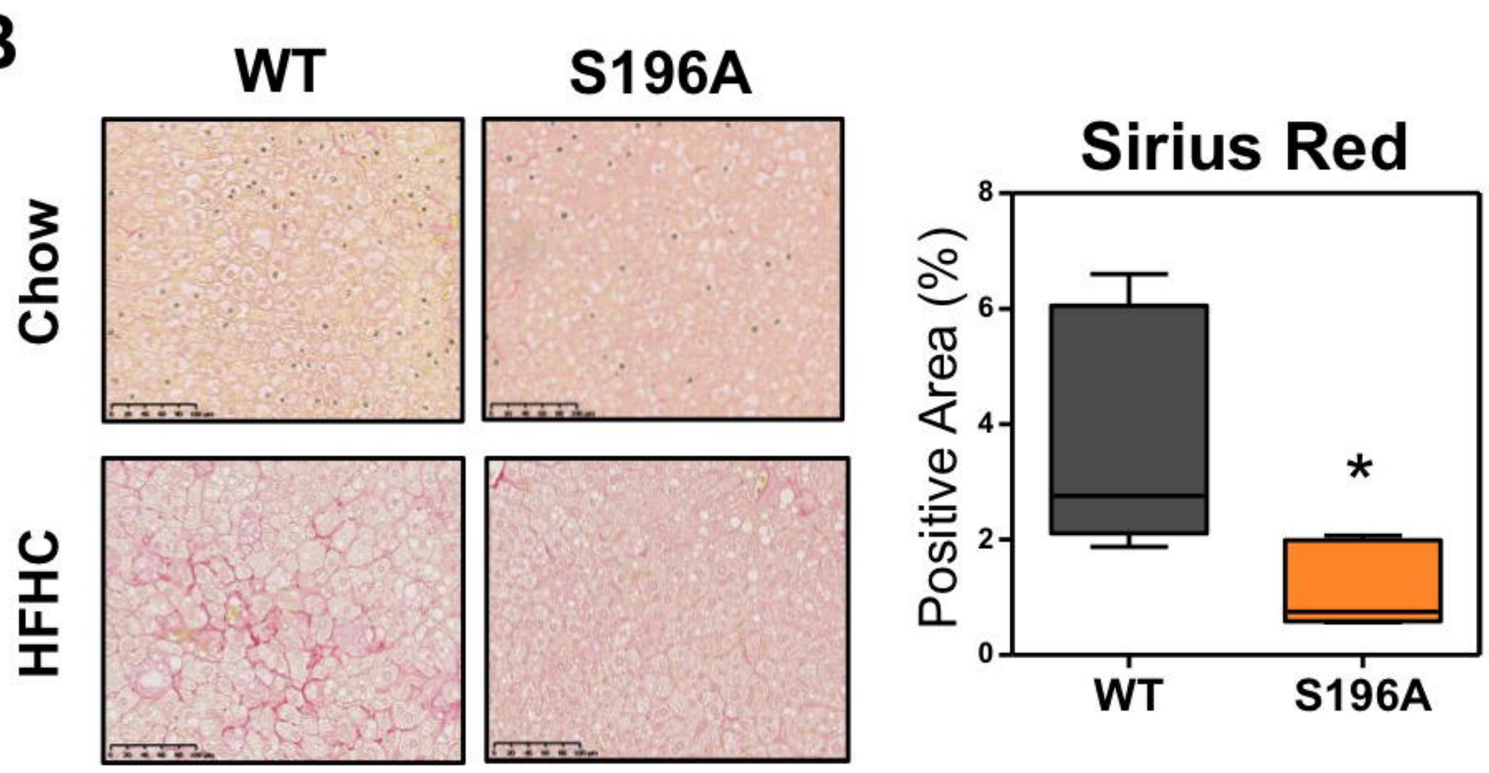

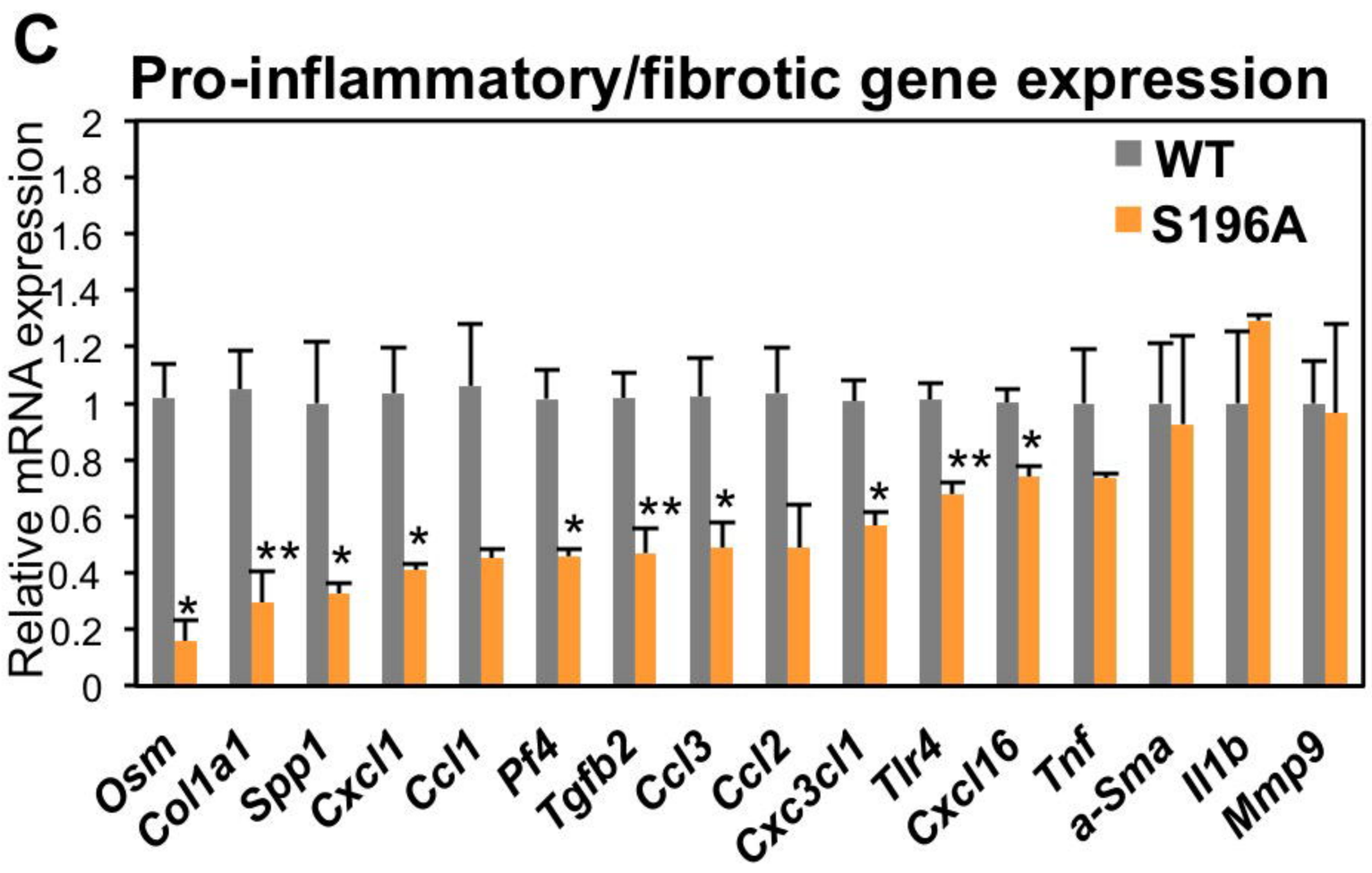

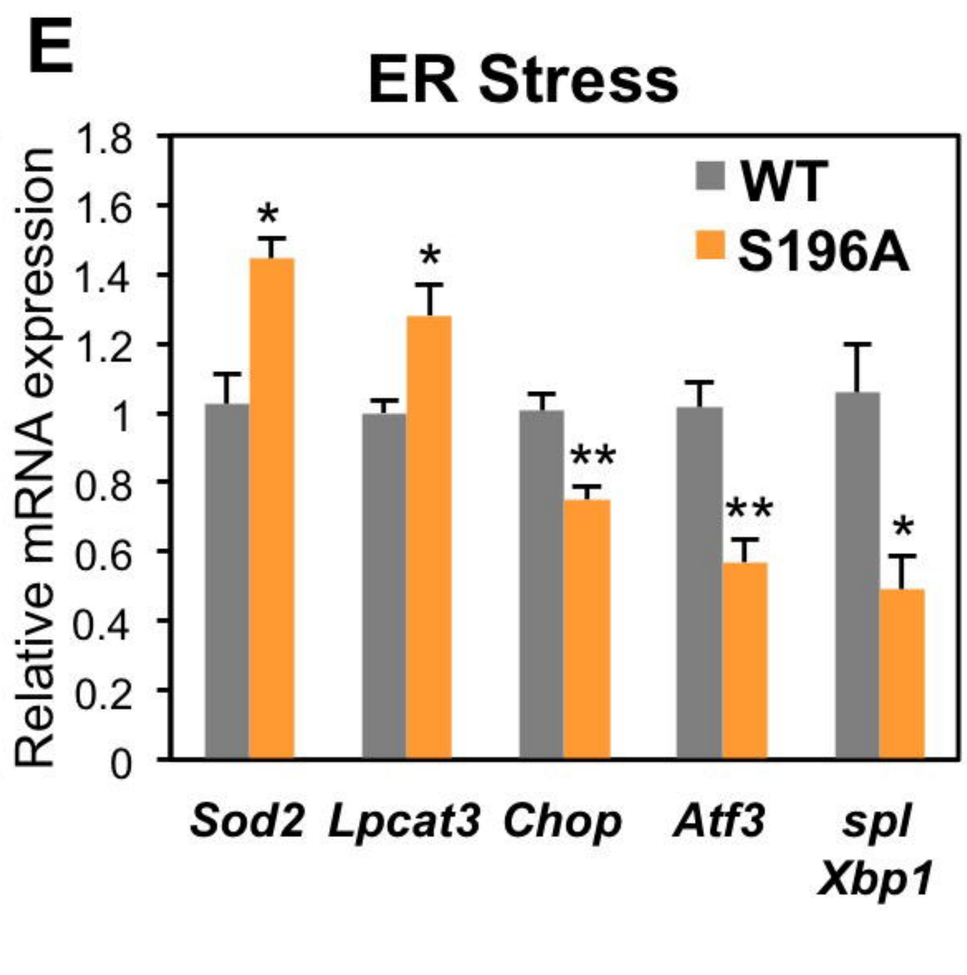

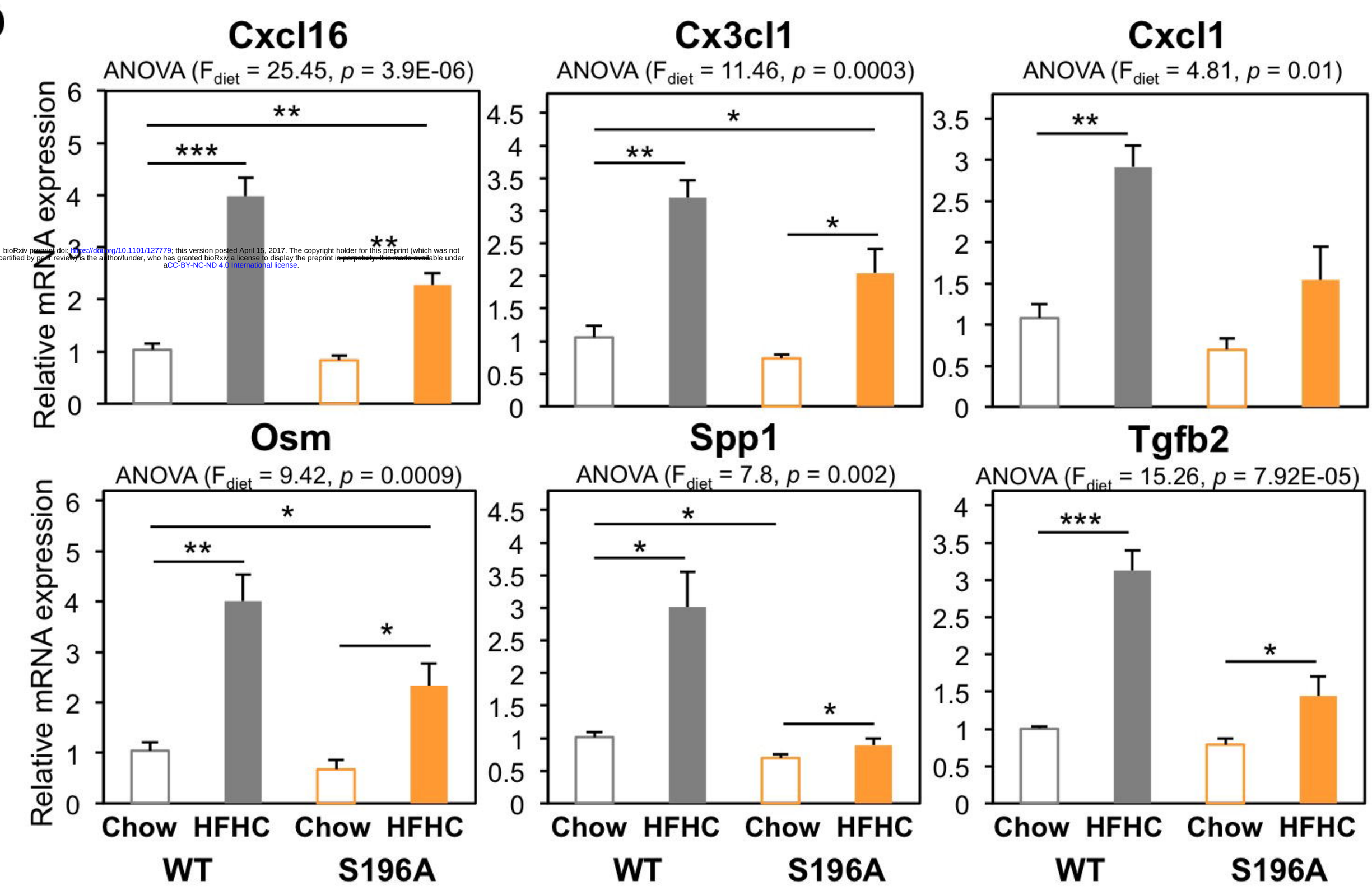

Figure 3

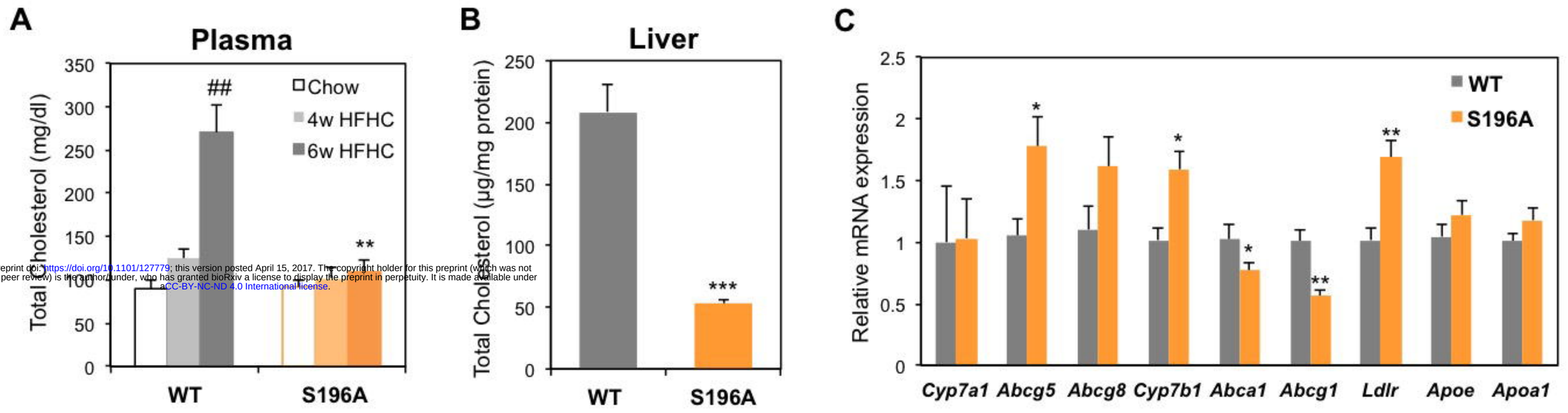

Figure 4